ISSN 1063-7788, Physics of Atomic Nuclei, 2020, Vol. 83, No. 2, pp. 285–289. © Pleiades Publishing, Ltd., 2020.

ELEMENTARY PARTICLES AND FIELDS
Experiment

Measurements of Cosmic Ray Muon Distributions with IceTop and IceCube

K. Rawlins*
(for the IceCube Collaboration)

University of Alaska Anchorage, Anchorage, AK 99508, United States
Received July 15, 2019; revised July 15, 2019; accepted July 15, 2019

Abstract—The IceTop detector is the surface component of the IceCube Observatory: an array of 81 "stations" of two frozen water tanks. Each tank contains two photosensors, and is sensitive to both the electromagnetic component of cosmic ray air showers as well as surface muons. While the electromagnetic component dominates in tanks close to the shower core, the signals from muons become more pronounced at large distances and at high zenith angles. Additionally, the deeply-buried in-ice component of IceCube can measure the high-energy penetrating muons from air showers. Together, these detectors can study the distributions of these air shower muons, and by comparing to the predictions of various hadronic interaction models, use them to constrain these models.

DOI: 10.1134/S1063778820020246

1. INTRODUCTION

Cosmic ray air showers contain different particle components which can be detected by many different detector technologies. The IceCube Neutrino Observatory [1] in particular is capable of studying these showers through several of these separate components. The deeply-buried "in-ice" detector can detect TeV muons from cosmic ray air showers, while the IceTop detector deployed at the surface above [2] is sensitive to both the electromagnetic and the GeV muon components. The proportions and properties of these components change with both primary energy and primary mass; for instance, iron-induced showers are more "muonic" than proton-induced showers. This makes an analysis of the muon component, separately from the electromagnetic component, potentially a powerful composition-sensitive tool [3]. Additionally, the high-energy muon component offers a window into the contribution from "prompt" particles early in the air shower development [4, 5].

However, predictions of these measurements also depend on hadronic interaction models, which are fraught with uncertainties. Their forward physics is difficult to test experimentally in accelerators. Several models are available, and one of the main differences in the predictions they make is in the number of both GeV muons at the surface and TeV muons at depth [6]. Therefore, muon measurements by both detectors are invaluable for testing and constraining these models.

*E-mail: krawlins@alaska.edu

2. GeV MUONS IN IceTop

The IceTop surface detector component of IceCube consists of 81 "stations" of two frozen water tanks each. Each tank holds two light-sensitive Digital Optical Modules (DOM's). The two tanks within a station are 10 m apart, and the stations themselves are positioned at the tops of IceCube strings, approximately 125 m apart on a triangular grid. When both tanks in a station record a trigger within a 1-μs window, both charges are read out as "Hard Local Coincidence" or HLC. When only one tank records a trigger, it is read out as a "Soft Local Coincidence" or SLC. Signals in tanks are expressed in units of "Vertical Equivalent Muons" or VEM.

Each tank is sensitive to the Cherenkov light deposited in the tank by charged particles, either from the electromagnetic component of the air shower or the muonic component. Single particle identification based on individual tank signals is not possible. However, the electromagnetic and muonic components have different lateral distribution behavior, with the muon lateral distribution extending out to much further distances. In addition, muon-induced signals are expected from single muons, whereas electromagnetic signals come from a broader smear of many particles. This can be seen in Fig. 1*a*, where the muons are responsible for the "thumb" structure at approximately 1 VEM, which becomes distinguishable from the EM background at large distances from the shower core.

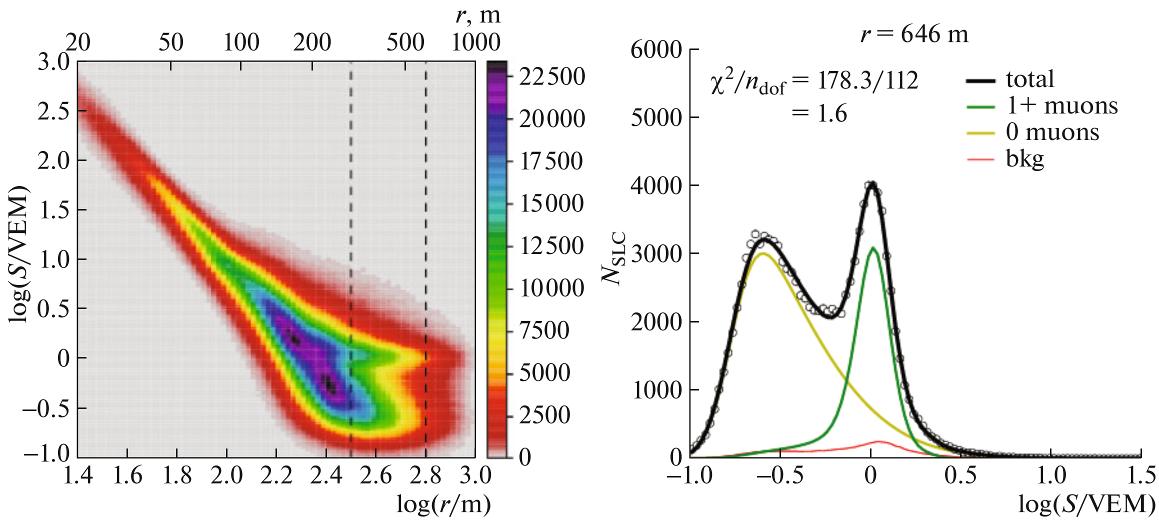

Fig. 1. (*a*) Signal deposited in tanks, as a function of radial distance from the shower core, for showers at one particular energy range (10–12.5 PeV) and zenith angle $\theta < 18°$. (*b*) Sample charge distributions from a "slice" of Fig. 1 at 646 m.

GeV muons have been studied using 3 years of data from the IceTop detector: one year from the 73-station configuration (IT-73) and two from the 81-station configuration (IT-81), from May 2010 to May 2013, with a lifetime of 947 days [7]. A series of quality cuts was applied, to restrict the sample to those that likely landed inside the physical extent of the detector and were reconstructed well. Additionally, this work used "near-vertical" events only ($\theta < 18°$), so as to make the muon tails the most easily visible. This work also includes SLC information as well as HLC information, since muons are more likely to trigger just one tank in a station and not the other.

2.1. Analysis

IceTop showers are reconstructed using a phenomenological model of both the charge lateral distribution function (LDF) and the shape of the shower front. Both charge and timing information from HLC hits are used to reconstruct the air shower's core position, direction, and the parameter S_{125} which is the signal at a reference distance of 125 m [2]. S_{125} is a proxy for the primary energy, and can be converted into $\log_{10}(E)$ using a function derived for measuring the all-particle cosmic ray spectrum using an H4a composition assumption [8].

Once each event is fit, the distributions such as the one shown in Fig. 1*a* can be sliced into bins of radius, and within each radius bin, forming charge distributions such as the ones shown in Fig. 1*b*. Each charge distribution is fit to a semi-analytical model containing three separate components: an EM component, a muon component, and a background from accidental coincidences. The EM component is modeled as a power law, modulated by threshold behavior at small signals. The muon component is modeled as a integer number of VEMs, modulated by geometric effects: both the change in the visible track length due to the angle of travel of the muon through the tank, and the possibility that the muon "clipped a corner" of the tank and deposited less than one VEM. Although many hits due to accidental coincidences are removed by considering their timing and making sure it is consistent with the rest of the shower, a contribution to the signal distribution from surviving accidental background is also included.

Fitting each slice in radius in this way, allows to fit a variety of free parameters, including (most importantly for this work), the mean number of muons $\langle N \rangle$ at that distance, which can be divided by the cross-sectional area of the tanks to express it as a muon density. Such muon densities are measured at many different distances, and for many different cosmic ray primary energies, as is shown in Fig. 2*a*.

2.2. Monte-Carlo Simulations

When the procedure described above is applied to IceTop data, a measured muon density at various distances can be pulled directly from the data, independent of any particular hadronic interaction model. However, translating this measurement into a *true* muon density requires a detailed understanding of systematic effects that can be seen in simulations. Thus, interpreting this result in the context of different cosmic ray composition and hadronic interaction models will require comparison to simulations as well.

Monte-Carlo simulations are created using CORSIKA [9], whose particles are then propagated

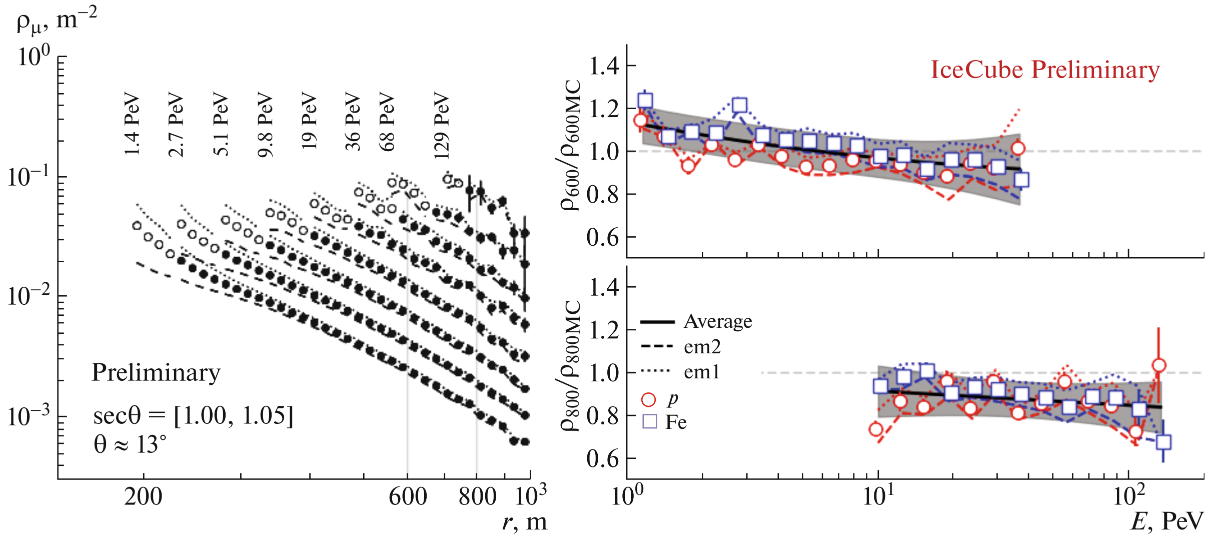

Fig. 2. (a) Measured muon densities, at a variety of different radial distances and primary energies. The dashed and dotted lines represent a systematic uncertainty from the model of the non-muon component of the signal. Open markers indicate data points we ignore due to this uncertainty. (b) Correction factors (ratio of measured muon density to true) for SIBYLL2.1 simulations. "EM1" and "EM2" refer to two different models of the electromagnetic signal used for fitting, such as in Fig. 1b. The solid black curve (average of proton and iron) is used to correct data for the final result, and the grey band is an estimate of the systematic uncertainty.

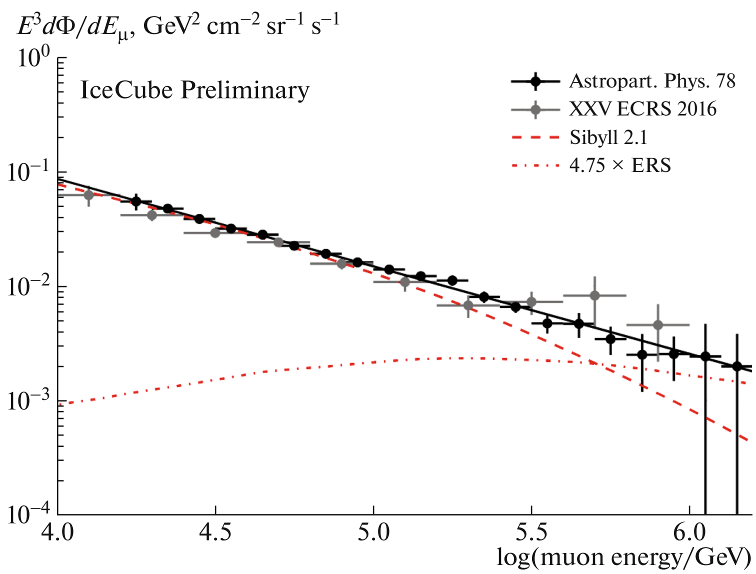

Fig. 3. All-sky muon energy spectrum measured in [4] and [5], compared to prediction from a pure conventional model with no prompt component (SIBYLL2.1) and to a model of prompt contribution (4.75 × ERS). From [15].

to a detector simulation based on GEANT4 [10]. For this work, simulated air showers are generated using a variety of different hadronic interaction models, including SIBYLL2.1 [11] (processed with full simulation, as a baseline), and SIBYLL2.3 [12], QGSJET-II-04 [13], and EPOS-LHC [14] (used to study model-dependent systematics). Since this analysis uses SLC hit informaion, particular attention was paid to simulating accidental coincidences, which appear most often in SLC's.

In these simulations, the *true* muon density at various distances can be extracted. When compared to the muon density measured using the fitting technique described above, systematic discrepancies can be observed. These discrepancies are the combined effects of various systematics present, such as: irregular snow coverage over the detector (which af-

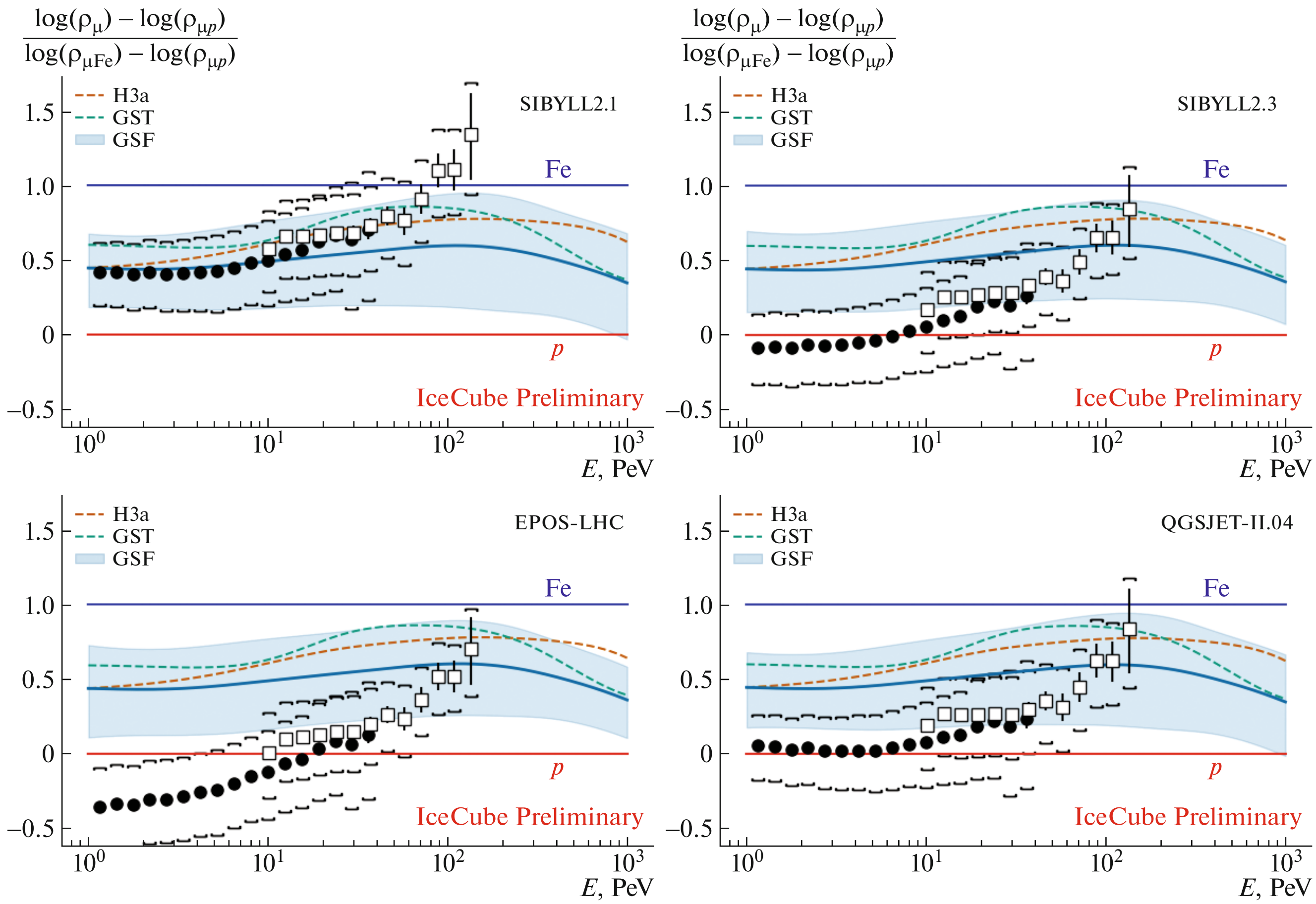

Fig. 4. Muon densities measured at 600 (closed circles) and 800 m (open squares), normalized by the logarithm of the density such that pure protons are zero and pure iron is one. Three composition models (H3a, GST, and GSF) are also plotted for comparison.

fects threshold behavior of EM signals), inaccuracies in the reconstructed shower track (which can cause bin migration in radius) or in reconstructed energy (which can cause bin migration in energy). To disentangle these systematics and correct for them, the reconstructed muon density can be divided by the true muon density to derive a "correction factor" for muon densities in data; such a correction factor (for SIBYLL2.1) is shown in Fig. 2*b*, and similar correction factors can be derived for the other hadronic interaction models. Since the correction factor is different for different nuclei, a composition model must be assumed; the average of the proton and iron correction factors is used here. Correction factors also differ between models, but the differences are small and the SIBYLL2.1 correction factor is used in the final analysis.

3. TeV MUONS IN IceCube

Below IceTop, the main "in-ice" detector of IceCube consists of 86 strings of DOM's, deployed at depths between 1450 and 2450 m, where TeV muons from cosmic ray air showers can penetrate. Although downgoing cosmic ray muons are a background for IceCube's flagship neutrino searches, they are also a tool for studying cosmic rays and shower physics. In particular, the energy spectrum of high-energy muons is expected to contain contributions from both a "conventional" flux and a "prompt" flux from short-lived heavy hadrons and mesons which decay early. The prompt flux is expected to become visible over the conventional flux in the high-energy tail of the muon spectrum, at around 1 PeV.

IceCube can map the energy deposition of downgoing muons as a function of slant depth in the ice, and the energy loss profile can be parametrized as a combination of a continuous energy loss and stochastic losses from particularly energetic particles. In the work described in [4], particularly large radiative energy losses are used to identify and estimate the energy of the highest-energy muons in events. An updated version of this same analysis approach, described in [5], uses machine learning to refine measurements of muon energy. The spectrum of these particles is then measured and compared to predictions from various models.

There are many systematic effects that can affect such a measurement, including (of course) the composition model that one has to assume, the properties of the ice, and the hadronic interaction model details of the simulations one compares to. Many of these effects (including the presence or absence of a prompt component) can be seen in zenith angle distributions, so these have been studied in some detail. The measured spectrum and its implications are discussed below.

4. RESULTS AND DISCUSSION

The spectrum of TeV muons from IceCube, as described above and measured in two different ways, is shown in Fig. 3. From this, we can observe that the muon spectrum is inconsistent with models that do *not* include any prompt component. Using the ERS flux [16] as a unit of measure for the prompt component, this analysis yields an estimate of the prompt flux of 4.75 × ERS, however this is given an assumption of a composition model (in particular, H3a), and is subject to myriad additional sources of systematic uncertainty that can swing this result from less than 1.0 ERS to nearly 7.0 ERS. Analysis such as these are dominated by uncertainties in primary flux (including the composition model), rather than in the hadronic interaction model.

The muon density at 600 m can be measured for showers with energies from 1–40 PeV, and at 800 m for 9–120 PeV. In Fig. 4, these muon densities have been interpreted for comparison to various hadronic interaction models by: a) applying the correction factor (depicted in Fig. 2*b*), and b) normalizing within each model in such a way as to put pure protons at zero and pure iron at one [17],

$$z = \frac{\log(\rho_\mu) - \log(\rho_{\mu,p})}{\log(\rho_{\mu,Fe}) - \log(\rho_{\mu,p})}.$$

The QGSJET-II.04 and SIBYLL2.1 models both are consistent with the muon density results, meaning that the measured muon density in data is bracketed by the expectations for protons and iron. SIBYLL2.3 is consistent with data only for 100% protons between 1–10 PeV. And EPOS-LHC is inconsistent with the data, requiring cosmic rays to be lighter than protons from 1–2 PeV, and is disfavored. The shape of these muon density curves does not match the expectation from composition models (such as H3a, GST, or GSF) in any of the hadronic interaction models; where a model seems to underpredict the muons in one energy range, it may be overpredicting in another.

Now, shifts in the energy scale of measurements could cause discrepancies in muon density such as is observed here, a vulnerability of all experiments including IceTop. In light of this shared concern, multi-experiment efforts are underway to compare systematics and energy scales, and explore the effects of aligning different experiments' energy scales to each other [6].

REFERENCES

1. A. Achterberg et al. (IceCube Collab.), Astropart. Phys. **26** 155 (2006).
2. R. Abbasi et al. (IceCube Collab.), Nucl. Instrum. Methods A **700**, 188 (2013).
3. M. G. Aartsen et al. (IceCube Collab.), Phys. Rev. D **100**, 082002 (2019).
4. M. G. Aartsen et al. (IceCube Collab.), Astropart.Phys. **78**, 1 (2016).
5. T. Fuchs et al. (IceCube Collab.), in Proceedings of the 25th ECRS, Turin, 2016 (2017); arXiv:1701.04067 [astro-ph.HE].
6. H. Dembinski et al. (EAS-MSU, IceCube, KASCADE-Grande, NEVOD-DECOR, Pierre Auger, SUGAR, Telescope Array, and Yakutsk Collabs.), in Proceedings of UHECR, 2018 (2019); arXiv:1902.08124 [astro-ph.HE].
7. J. Gonzalez et al. (IceCube Collab.), in Proceedings of ISVHECRI, Japan, 2018, EPJ Web Conf. **208**, 03003 (2019).
8. T. K. Gaisser, Astropart. Phys. **35**, 801 (2012).
9. D. Heck, J. Knapp, J. N. Capdeviell, G. Schatz, and T. Thouw, *CORSIKA: A Monte Carlo Code to Simulate Extensive Air Showers*, FZKA 6019 (Forschungszentrum Karlsruhe, 1998).
10. S. Agostinelli et al. (Geant4 Collab.), Nucl. Instrum. Methods A **506**, 250 (2003).
11. E. J. Ahn, R. Engel, T. K. Gaisser, P. Lipari, and T. Stanev, Phys. Rev. D **80**, 094003 (2009).
12. F. Riehn, R. Engel, A. Fedynitch, T. K. Gaisser, and T. Stanev, EPJ Web Conf. **99**, 12001 (2015).
13. S. Ostapchenko, Nucl. Phys. B Proc. Suppl **151**, 143 (2006).
14. T. Pierog et al., Phys. Rev. C **92**, 034906 (2015).
15. D. Soldin et al. (IceCube Collab.), in Proceedings of ISVHECRI, 2018, EPJ Web Conf. **208**, 08007 (2019); arXiv:1811.03651 [astro-ph.HE].
16. R. Enberg, M. Reno, and I. Sarcevic, Phys. Rev. D **78** 043005 (2008).
17. S. deRidder et al. (IceCube Collab.), in Proceedings of the 35th ICRC, 2017 (2017); PoS(ICRC2017)319.